Journal of
Ceramic Science
and Technology

J. Ceram. Sci. Technol., **08** [2] 233-242 (2017)
DOI: 10.4416/JCST2016-00110
available online at: http://www.ceramic-science.com

Mechanical Properties, Strengthening and Toughening Mechanisms of Reactive-Hot-Pressed TiB_2-SiC-Ni Ceramic Composites

G. Zhao*[1], C. Huang[2], N. He[1], H. Liu[2]

[1]College of Mechanical and Electrical Engineering, Nanjing University of Aeronautics and Astronautics, Nanjing 210016, P. R. China
[2]Key Laboratory of High-efficien-cy and Clean Mechanical Manufacture (Shandong University), Ministry of Education, P. R. China

received November 14, 2016; received in revised form December 15, 2016; accepted February 21, 2017

Abstract

A TiB_2-SiC-5 wt %Ni ceramic composite with high flexural strength and fracture toughness was fabricated in the reactive hot pressing (RHP) process. Different sintering times and sintering temperatures were employed. The strengthening and toughening mechanisms were investigated in detail. The composition and microstructure were investigated by means of X-ray diffraction (XRD), scanning electron microscopy (SEM), transmission electron microscope (TEM) and energy-dispersive spectroscopy (EDS). The sintering time and sintering temperature had a significant influence on the mechanical properties and microstructure of the composite. The mechanical properties decreased as the sintering time was increased from 30 to 45 min, and subsequently increased with the further increase of the sintering time. The mechanical properties of the composite increased gradually as the sintering temperature increased. For the investigated range of parameters, the composite prepared at 1700 °C for 30 min had the optimum comprehensive mechanical properties with flexural strength of 1121 ± 31 MPa, fracture toughness of 7.9 ± 0.58 MPa·m$^{1/2}$ and hardness of 21.3 ± 0.62 GPa. The improved flexural strength and fracture toughness of the composite were attributed to the strengthening and toughening effects of Ni and the elongated TiB_2 grains, the intragranular nano-particle structure, and the dislocations and stacking fault. The clean interface is also conducive to the improved flexural strength.

Keywords: TiB_2-SiC-Ni composite, mechanical properties, microstructure, reactive hot pressing, strengthening and toughening mechanism.

I. Introduction

Titanium diboride (TiB_2) has an excellent combination of properties including high hardness and elastic modulus, high melting point, good abrasive resistance, superior thermal and electrical conductivity [1]. These properties make it ideally suited for high-temperature structural applications such as cutting tools, armor and wear parts [2]. However, the comparatively high vapor pressure of the constituents and the low self-diffusion coefficient of TiB_2 result in difficult densification. Extremely high sintering temperatures up to 2000 °C and a long dwell time are required to get fully dense monolithic TiB_2 ceramics. Such processing conditions lead to exaggerated grain growth of the as-sintered materials, resulting in degradation of the mechanical properties. Spark-plasma sintering (SPS) and microwave sintering (MWS) are alternative methods for consolidation of monolithic TiB_2 ceramics with a relatively low temperature and short dwell time [3–5]. However, the mechanical properties and elastic modulus of the TiB_2 ceramics fabricated with these methods are relatively low and inadequate for many structural applications.

In order to overcome the densification problem, various metallic and non-metallic additives have been used to obtain dense TiB_2-based ceramics. The flexural strength of TiB_2 at room temperature can be significantly enhanced with the addition of Ni as binder [6–7]. In addition, it has been confirmed that the mechanical properties and oxidation resistance of TiB_2 can be improved with the addition of SiC [8]. TiB_2-SiC ceramic composite can be fabricated by means of different densification techniques. Shiro *et al.* [9] prepared TiB_2-SiC ceramic composites with 1 – 10 wt% SiC using pressureless sintering (PS) and hot isostatic pressing (HIP) methods. Zhu *et al.* [10] prepared TiB_2-SiC ceramic composite with 96 % density in an *in-situ* HIP process. However, the fracture toughness of the composites prepared with these methods was lower than 5 MPa·m$^{1/2}$. Chen *et al.* [11] first used the high-frequency induction heating method to fabricate TiB_2-SiC composite and the mechanical properties were relatively high. In our previous study, TiB_2-SiC ceramic composites with relatively high fracture toughness were prepared using the hot pressing (HP) method [12]. Reactive hot pressing (RHP) is an *in-situ* technique that can be used to fabricate ceramic composites at relatively low temperatures. As well as the low-temperature processing, the advantages of the RHP method consist of increased control over microstructure development and properties, and the use of

* Corresponding author: zhaogl@nuaa.edu.cn

cheaper, more abundant precursors [13]. A variety of ceramic composites including ZrB_2-SiC, TiB_2-SiC, ZrB_2-$MoSi_2$, Al_2O_3-$MoSi_2$ have been prepared with the RHP method[14–17]. The mechanical properties of these composites were superior to composites with the same composition but prepared with the conventional process. Particularly, TiB_2-based ceramic composites with *in-situ* synthesized elongated TiB_2 grains can be prepared using the RHP process [18]. The microstructure of the composites is different from those prepared in the non-RHP process (PS, HP and HIP) and the mechanical properties are improved.

Up to now, very few reports on the microstructure and mechanical properties of reactive-hot-pressed TiB_2-SiC ceramic composites with Ni as binder can be noted. In the present work, TiB_2-SiC ceramic composite with 5 wt% Ni as binder was synthesized *in-situ* in the RHP process. The effects of sintering times and sintering temperatures on the microstructure and mechanical properties of the composite were studied. The strengthening and toughening mechanisms of the composite were investigated in detail.

II. Experimental Procedure

(1) Materials preparation

The TiB_2-SiC-Ni ceramic composites were prepared by means of the RHP process according to the following reaction:

$$Si + 2Ti + B_4C + xNi \rightarrow 2TiB_2 + SiC + xNi \quad (1)$$

where x is the amount of nickel powder (mol) used as the additive. In the present work, x = 0.1606 was employed in order to maintain the theoretical content of Ni at 5 wt% in the ceramic composite. The starting materials were silicon, titanium, boron carbide and nickel powders. Their grain sizes and the purities provided by the suppliers are listed in Table 1. The titanium raw powder was firstly ball-milled in ethanol medium using tungsten carbide (WC) balls (8 – 10 mm) for 96 h at 325 rpm in order to break down any agglomerated particles, and then the powder was dried at 120 °C in a vacuum dry oven (Guang Ming) for further use. The stoichiometric powders were mixed and ball-milled using analytical-grade ethanol as the medium with WC balls (8 – 10 mm) for 48 h at 325 rpm in polyethylene jars. The ball-powder mass ratio was fixed at 10:1. After mixing, the slurry was dried in a vacuum dry oven at 120 °C and sieved through a 120-mesh sieve. Subsequently, the mixture was placed into a cylindrical graphite die and then reactive-hot-pressed at a heating rate of 50 K/min under a uniaxial pressure of 32 MPa in vacuum. Different sintering times and temperatures were employed. The sintered samples were in the form of 4.5-mm disks with a diameter of about 42 mm.

(2) Mechanical properties measurement

The reactive-hot-pressed disks were sectioned into several specimens with dimensions of 3 mm × 4 mm × 36 mm using an electrical discharge machine (EDM, DK7716). Subsequently, the surfaces of the testing bars were polished using polishing machinery (P-2) with diamond slurries (1 μm). The edges of all the samples were chamfered to minimize the stress concentration induced during the machining process. The flexural strength was measured in static air using a three-point tester (Instron, 8801) with a support span of 30 mm and a loading rate of 0.5 mm/min. The load was applied parallel to the pressing direction and the flexural strength was averaged from six specimens. The Vickers hardness was measured on the polished surface using a Vickers diamond pyramid indenter (HVS-50) with a static load of 196 N and a loading time of 15 sec. The values of the fracture toughness (K_{IC}) were calculated with Equation (2), reported by Fukuhara *et al.* [19]. The values of hardness and fracture toughness were calculated from the average of ten indentations.

$$K_{IC} = 0.203 H_V a^{1/2} \left[\frac{c}{a}\right]^{-3/2} \quad (2)$$

where H_V is the Vickers hardness, 2*a* is the length of the impression diagonal and 2*c* is the overall indentation crack length including 2*a*.

Table 1: Characteristics of the starting powders.

Powder	Purity	Particle size (μm)	Supplier
Si	99.9 %	1.0 ± 0.1	Shanghai St-Nano science and Technology Co., Ltd
Ti	99.5 %	45.0 ± 5.5	General Research Institute for nonferrous Metals
B_4C	99.0 %	7.0 ± 1.5	Jingangzuan Boron Carbide Co., Ltd
Ni	99.9 %	0.05	Shanghai St-Nano science and Technology Co., Ltd

(3) Characterization

The phase composition was characterized by means of X-ray diffraction (XRD) (Hitachi RAX-10A-X). CuKα1 radiation (λ=1.54050 Å) and a scan step of 0.2 °/min were used. The XRD peaks were identified by matching to the JCPDS-ICDD data cards. The fractured and polished surfaces were observed with an SEM (Auriga-60, ZEISS) equipped with an energy-dispersive spectrometer (EDS, Oxford). The characterization of the composite, including the distribution of the grains, interface, compositions and defects, was analyzed using a 200 kV TEM (JEM-2010F, JEOL) equipped with an X-ray energy-dispersive detector (EDS, EDAX). The TEM samples were prepared with a focused ion beam (FIB, Auriga-60, ZEISS) using the H-bar method.

III. Results and Discussion

(1) Phase identification

According to Equation (1), the TiB_2-SiC ceramic composites with different contents of Ni as binder can be prepared by changing the value of x, indicating that the microstructure and mechanical properties of the composites

can be tailored via the RHP process. In the present study, the theoretical mass fractions of TiB_2 and SiC were 73.7 % and 21.3 % respectively, thus TiB_2 and SiC can be treated as the matrix and secondary-phase particles respectively. The XRD pattern of the composite prepared at 1700 °C for 30 min is shown in Fig. 1. TiB_2-SiC-Ni ceramic composite was successfully synthesized *in-situ* with the RHP process using Si, Ti, B_4C and Ni as raw materials. Except for TiB_2, SiC and Ni, no other phases with significant peak intensity were found, demonstrating that the reaction took place in accordance with Equation (1) and a full conversion of reagents into products was achieved. In the literature [20], the brittle phase of Ni_3B_4 was found in the TiB_2-based ceramic composite prepared with the HP process. The brittle phase was ascribed to the reaction between TiB_2 and Ni, and decreased the mechanical properties of the composite. However, in the present work, no brittle phase was detected, indicating that Ni was more stable in the ceramic composite prepared with the RHP process. This is one of the advantages of RHP as a sintering method to form ceramic composites.

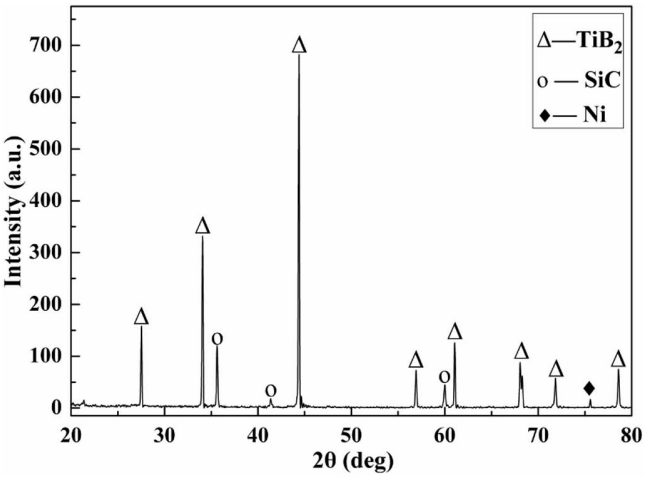

Fig. 1: XRD pattern of the TiB_2-SiC-Ni ceramic composite.

The SEM micrograph of the polished surface of the composite prepared at 1700 °C for 30 min and the corresponding EDS mapping are shown in Fig. 2. Three kinds of materials with different backscattered electron contrast were observed on the polished surface. The EDS mapping revealed that the dark contrast was SiC, the gray contrast was TiB_2 and the bright contrast was Ni. The network-structured SiC was distributed in the TiB_2 matrix and the microstructure of the composite was heterogeneous with clusters of TiB_2 grains. Ni as binder was mainly distributed in the interfaces of TiB_2-SiC and TiB_2-TiB_2 rather than the interface of SiC-SiC, which resulted in the drop of SiC grain from the polished surface as shown in Fig. 2.

(2) Effect of sintering time on the mechanical properties and microstructure

The effect of the sintering time on the mechanical properties of the TiB_2-SiC-5 wt%Ni ceramic composite prepared at 1700 °C is shown in Fig. 3. It can be seen that the flexural strength, fracture toughness and hardness decreased as the sintering time increased from 30 to 45 min, and subsequently increased with the further increase of the sintering time. For the investigated range of parameters, the composite prepared at 1700 °C for 30 min had the optimum comprehensive mechanical properties with flexural strength of 1121 ± 31 MPa, fracture toughness of 7.9 ± 0.58 MPa·$m^{1/2}$ and hardness of 21.3 ± 0.62 GPa. The mechanical properties of the TiB_2-SiC-5 wt%Ni ceramic composite were higher than that of the TiB_2-SiC ceramic composite prepared in our previous study [18]. A TiB_2-SiC ceramic composite with higher hardness (28.6 GPa) was fabricated using the RHP process by Zhang *et al.* [15]. However, the flexural strength and fracture toughness in their paper were only about 654 MPa and 6.8 MPa·$m^{1/2}$ respectively, which was lower than that in the present study. In addition, the flexural strength and fracture toughness of the TiB_2-SiC ceramic composites reported in other studies were relatively low (less than 700 MPa and 7 MPa·$m^{1/2}$ respectively). Therefore, the addition of Ni as a binder improved the mechanical properties of the composite significantly. The composite prepared at 1700 °C for 45 min had relatively low mechanical properties with flexural strength of 864 ± 25 MPa, fracture toughness of 6.7 ± 0.51 MPa·$m^{1/2}$ and hardness of 20.0 ± 0.71 GPa. The flexural strength was still higher than that of the TiB_2-SiC composites without Ni as additive.

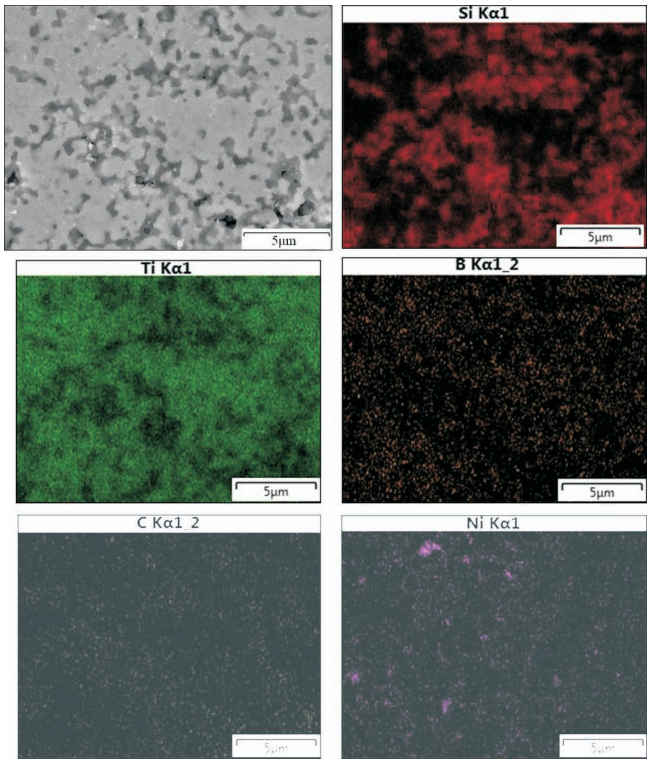

Fig. 2: SEM image of the polished surface and the EDS mapping.

The SEM images of the fractured surfaces of the composite prepared at 1700 °C for different sintering times are shown in Fig. 4. It can be seen from Fig. 4(a) that the grains size was less than 3 μm, indicating that a ceramic composite with a fine microstructure could be synthesized with the RHP process using starting powders with larger particle size. The fracture of the composite sintered for 30 min was characterized by a mixed mode of intergranular and

transgranular fracture, which enhanced its fracture toughness. It was difficult to observe pores on the fractured surface, indicating a high relative density. As a result, the flexural strength and hardness of the composite increased. As the sintering time increased to 45 min, a few large grains (> 5 μm) were observed, as shown in Fig. 4(b). Moreover, a number of pores were distributed in the composite, indicating a low relative density. As a result, the flexural strength and hardness of the composite decreased. Exaggerated grain growth was found on the fractured surface shown in Fig. 4(c). According to Hall-Petch relationship, the flexural strength decreased as the grain size increased. Few pores can be observed in the composite, indicating a high relative density. Thus the composite possessed a relatively high hardness. The fracture mode was a mixed mode of intergranular and transgranular fracture, which improved the fracture toughness of the composite.

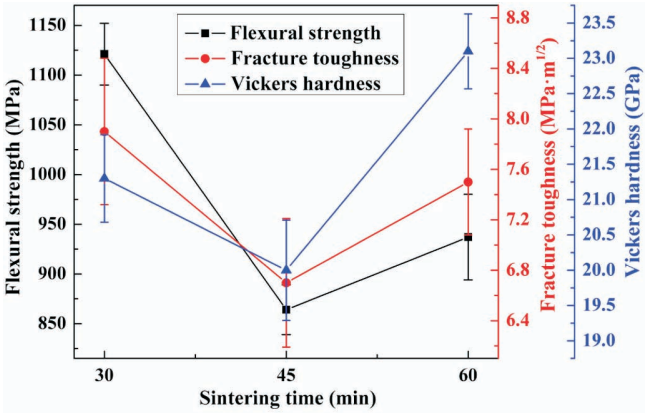

Fig. 3: Effect of sintering time on the mechanical properties of the composite sintered at 1700 °C.

(3) Effect of sintering temperature on the mechanical properties and microstructure

<?texbefel ?>The effect of the sintering temperature on the mechanical properties of the TiB_2-SiC-5 wt% Ni ceramic composite sintered for 30 min is shown in Fig. 5. The flexural strength, fracture toughness and hardness increased gradually as the sintering temperature increased. For the investigated range of parameters, the composite prepared at 1700 °C for 30 min had the optimum comprehensive mechanical properties with flexural strength of 1121 ± 31 MPa, fracture toughness of 7.9 ± 0.58 MPa·m$^{1/2}$ and hardness of 21.3 ± 0.62 GPa. The SEM images of the fractured and polished surfaces of the composite sintered at 1600 °C for 30 min are shown in Fig. 6. A number of pores can be observed on the fractured surface shown in Fig. 6(a), indicating a low relative density. In addition, the distribution of the SiC grains was heterogeneous and some grains dropped from the polished surface, as shown in Fig. 6(b). As a result, the flexural strength and hardness of the composite decreased. With a further increase of the sintering temperature to 1650 °C, it can be seen from Fig. 7(a) that the porosity decreased. Besides, the fracture mode was characterized by a mixed mode of intergranular and transgranular fracture, as shown in Fig. 7(b). As a result, the mechanical properties of the composite increased.

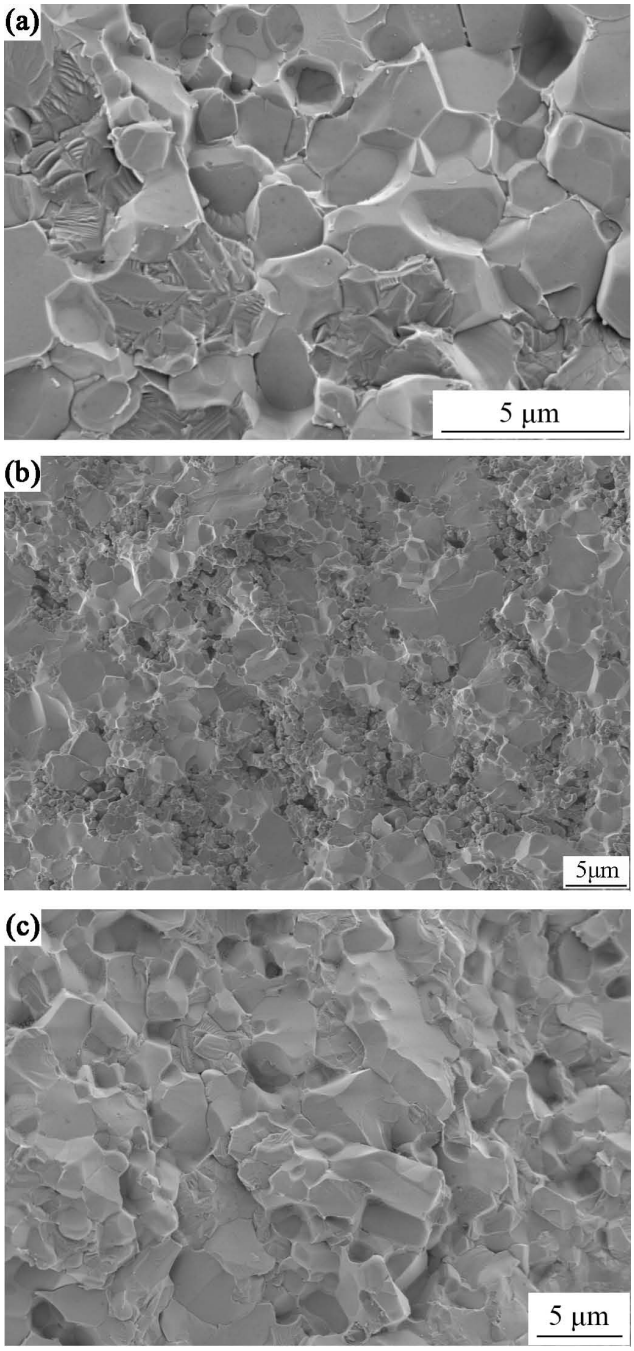

Fig. 4: SEM images of the fractured surfaces of the composites sintered for (a) 30, (b) 45 and (c) 60 min.

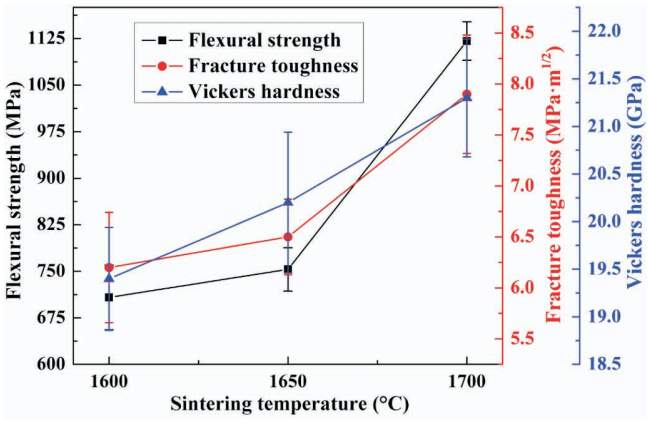

Fig. 5: Effect of sintering temperature on the mechanical properties of the composite sintered for 30 min.

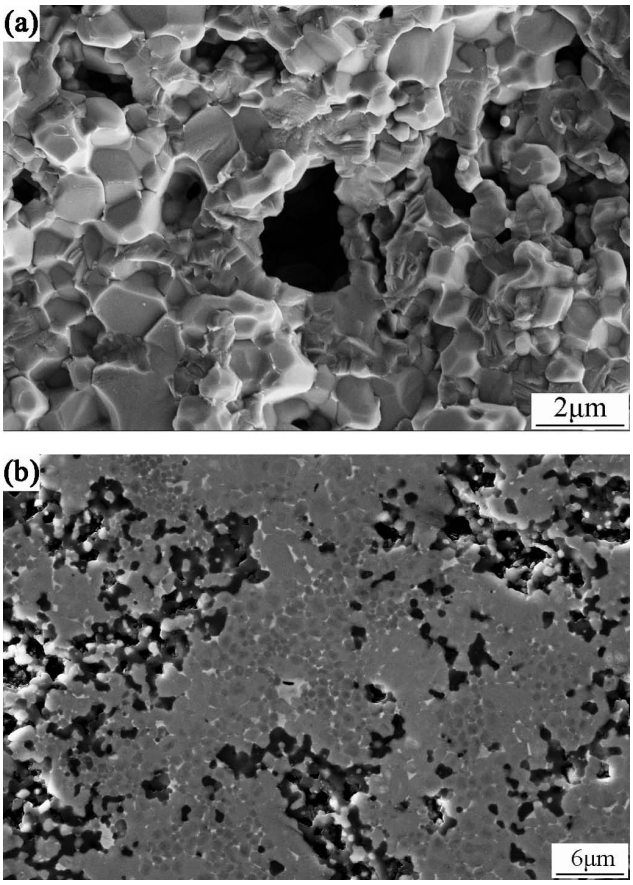

Fig. 6: SEM images of the (a) fractured and (b) polished surfaces of the composite sintered at 1600 °C.

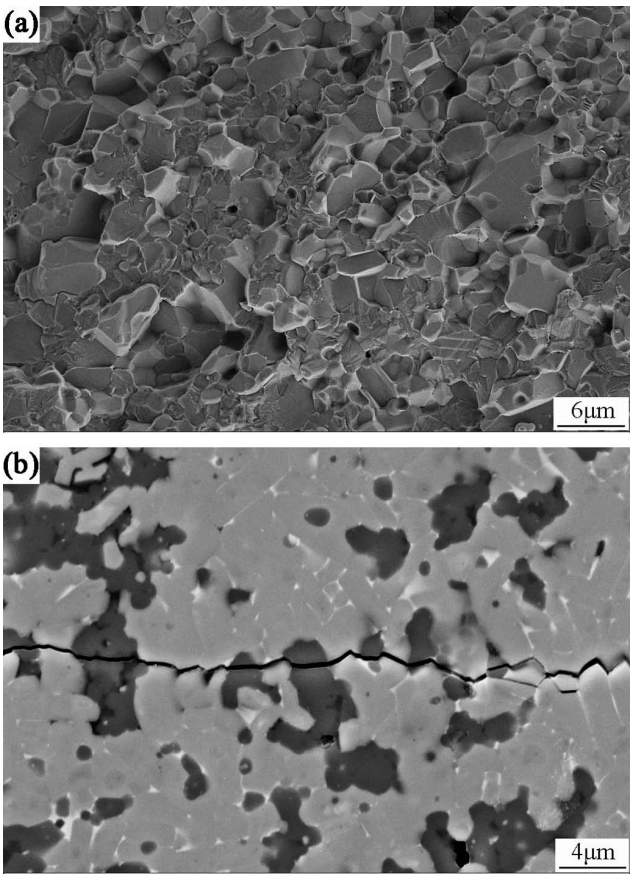

Fig. 7: SEM images of the (a) fractured and (b) polished surfaces of the composite sintered at 1650 °C.

(4) Strengthening and toughening mechanisms

Compared with the TiB_2-SiC ceramic composites prepared in our previous study [18], the flexural strength and fracture toughness of the TiB_2-SiC-5 wt% ceramic composite are significantly improved. Regarded in combination with the microstructural analysis, the strengthening and toughening mechanisms of the composite are discussed in detail.

First, the addition of Ni as binder is conductive to improving the flexural strength and fracture toughness of the composite. The STEM images of the composite prepared at 1700 °C for 30 min are shown in Fig. 8. The EDS patterns shown in Fig. 9(a-d) reveal that the gray, black and white phases are TiB_2, SiC and Ni respectively. It is seen from Fig. 8(a) that Ni is mainly distributed in the interfaces and triple grain junctions. As a result, the interface bond strength and the relative density are enhanced. In addition, the ductile phase toughening effect of Ni improves the fracture toughness of the composite. When the crack propagates to Ni in the composite, the ductile Ni contributes to the toughness by inhibiting crack opening. Simultaneously, the plastic straining of Ni causes crack shielding [21]. As a result, the fracture toughness of the composite is increased.

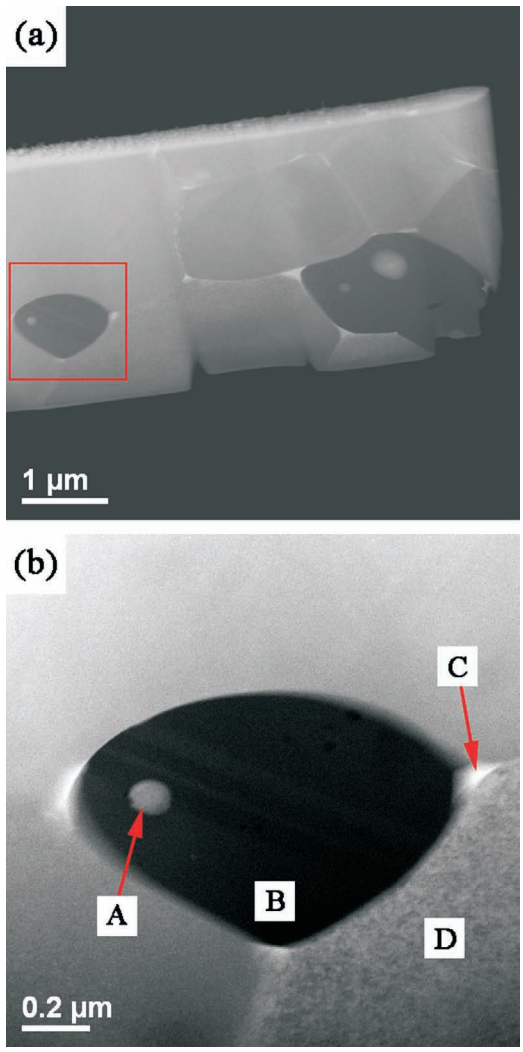

Fig. 8: STEM images of (a) the composite and (b) magnification of the frame region.

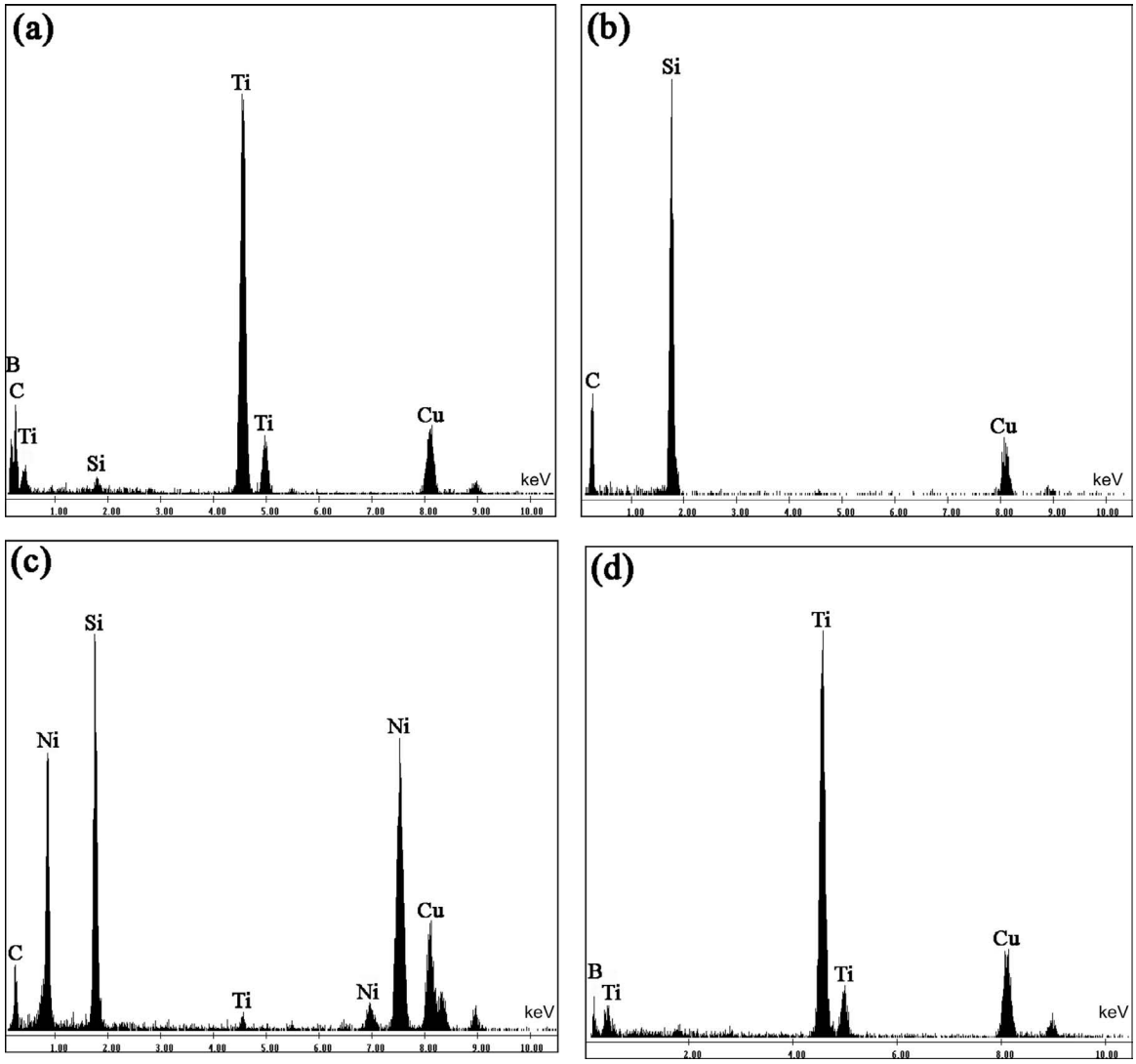

Fig. 9: EDS patterns of grains A-D shown in (b).

Second, the improved fracture toughness is attributed to the intragranular nano-particle structure. As shown in Fig. 8(b), an intragranular TiB_2 nano-particle is observed in SiC. The intragranular TiB_2 nano-particle can not only inhibit the grain growth of SiC, but also change the fracture mode of the composite. A schematic diagram of crack propagation in the composite is shown in Fig. 10. Owing to the mismatch of the thermal expansion coefficient between TiB_2 (4.6×10^{-6}/K) and SiC (4.02×10^{-6}/K), a weak interface exists. Thus the crack is prone to cross the SiC grain and reach the boundary between the intragranular TiB_2 nano-particle and SiC. As a result, more crack extension energy is consumed and the fracture toughness of the composite is increased.

Third, the improved flexural strength is also attributed to the clean interface. In the present work, because of the exothermic reaction (Equation (1)) in the RHP process, an extremely high temperature was generated during the reaction process. Therefore, the low-melting-point impurities vaporized, and a relatively clean interface was obtained. Fig. 11 shows the HRTEM image of the interface between the TiB_2 and SiC grains shown in Fig. 8(b). This kind of clean interface is conducive to improved flexural strength. Additionally, it is seen from the HRTEM image that the SiC grain is a single crystal. It is well-acknowledged that single crystal has high strength and elastic modulus. Thus more fracture energy is consumed when the crack crosses the SiC grain. As a result, the flexural strength and fracture toughness of the composite are increased.

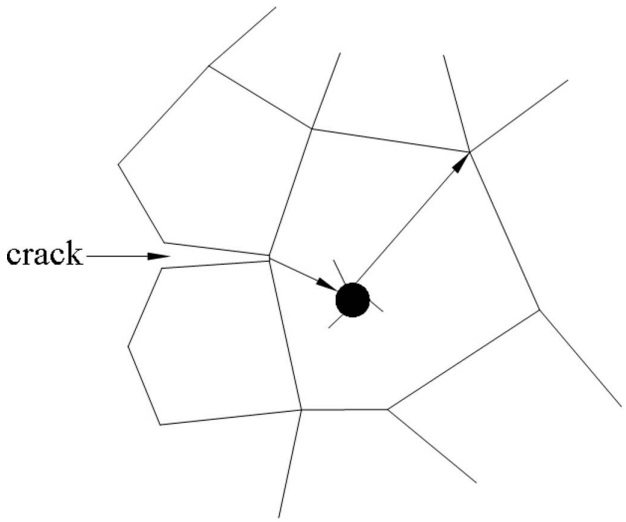

Fig. 10: Schematic diagram of crack propagation in the composite.

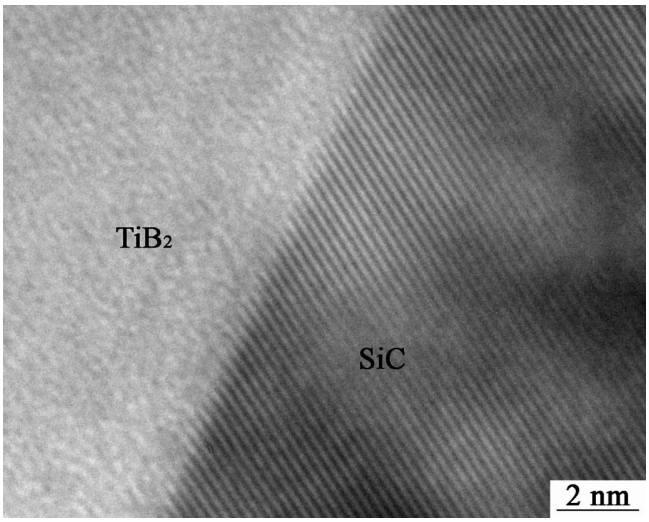

Fig. 11: HRTEM image on the interface between the TiB_2 and SiC grains.

The morphology of the polished surface of the composite is shown in Fig. 12(a). A number of elongated grains are randomly oriented and uniformly distributed in the composite. The elongated grains are 0.5 – 1.5 μm in diameter and 3 – 10 in aspect ratio. The EDS analysis shown in Fig. 12(b) reveals that the elongated grain is TiB_2. The improved flexural strength and fracture toughness of the composite are ascribed to the strengthening and toughening mechanisms of the elongated TiB_2 grains including crack deflection, crack bridging, crack branching, grain fracture and grain pullout, as discussed in our previous study [18]. In addition, specific microstructural features such as intragranular elongated grain, dislocations and stacking faults are also observed in the composite, as shown in Fig. 13 and Fig. 14. The HRTEM shown in Fig. 13(b) demonstrates that the elongated grain shown in Fig. 13(a) is a single crystal. The interlayer spacing measured from the image is about 3.3 Å, which is consistent with the lattice parameter of TiB_2. Similar to the strengthening and toughening mechanisms of the elongated TiB_2 grains discussed above, the intragranular elongated TiB_2 grain is also conducive to improved flexural strength and fracture toughness. When the crack reaches the dislocation or stacking fault areas, the dislocations or stacking fault in the matrix operates as nano-crack nuclei in the vicinity of the propagating crack tip [22]. The stress field near the crack tip is released by nano-crack nucleation and the fracture toughness and flexural strength of the composite are further increased.

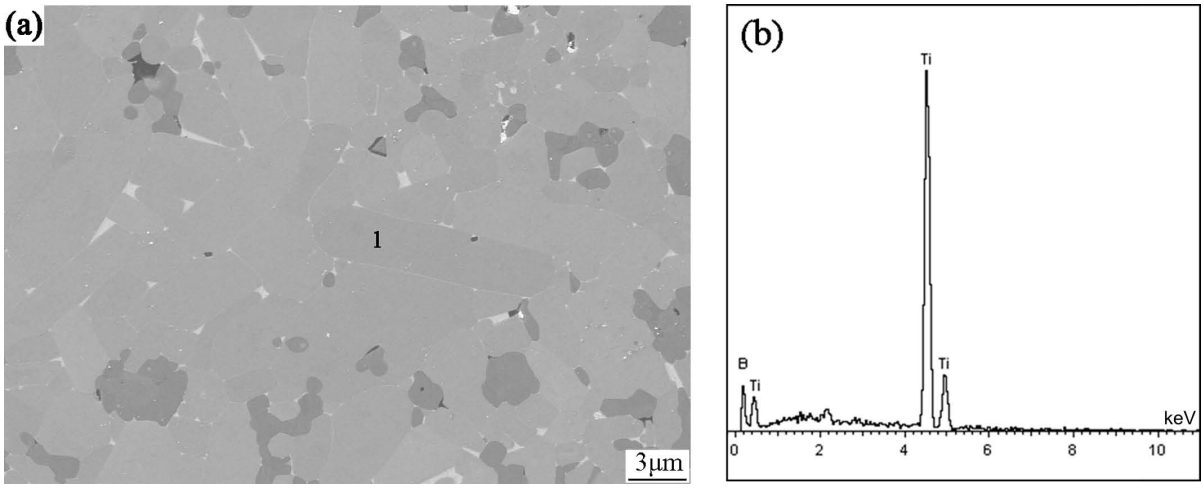

Fig. 12: The (a) SEM image on the polished surface and (b) EDS pattern of point 1.

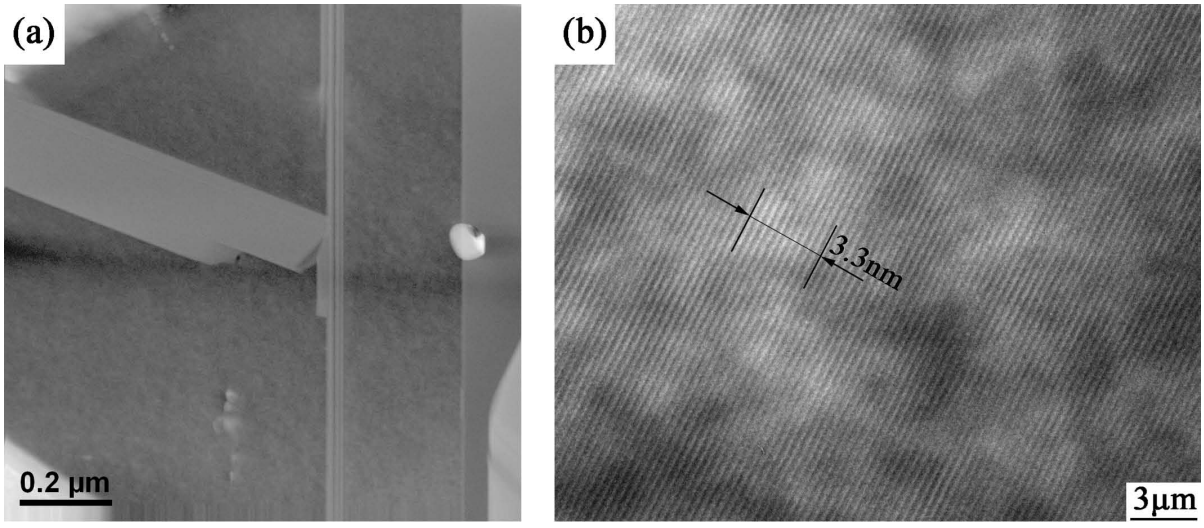

Fig. 13: The (a) STEM and (b) HRTEM images of an intragranular elongated grain.

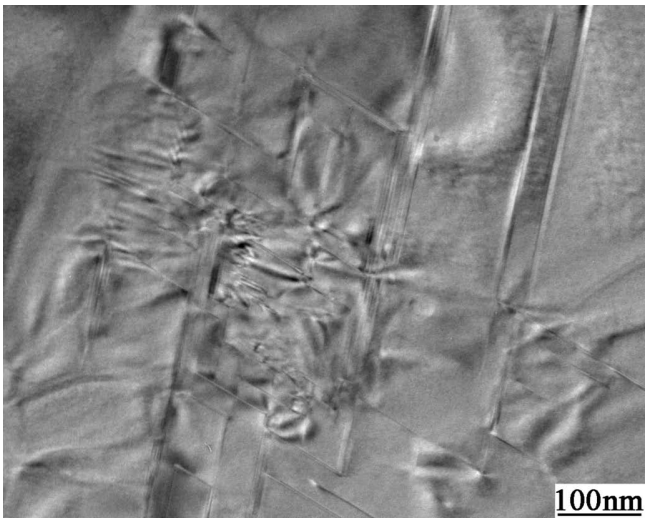

Fig. 14: TEM image showing the dislocations and stacking fault in the composite.

IV. Conclusions

(1) The TiB_2-SiC-5 wt% Ni ceramic composite was synthesized *in-situ* with the RHP process under 32 MPa in vacuum. Different sintering times and sintering temperatures were employed. The composition identified with X-ray diffraction (XRD) indicated that full conversion of reagents into products was achieved. The microstructure was investigated by means of scanning electron microscopy (SEM) and transmission electron microscopy (TEM) equipped with an energy-dispersive spectrometer (EDS).

(2) The sintering time and sintering temperatures had a significant influence on the mechanical properties and microstructure of the composite. The mechanical properties decreased as the sintering time increased from 30 to 45 min, and subsequently increased with the further increase of the sintering time. The composite prepared at 1700 °C for 45 min had relatively low mechanical properties because of the large grains and low density. The mechanical properties of the composite increased gradually as the sintering temperature increased. The composite prepared at 1600 °C for 30 min had relatively low mechanical properties because of the low density and heterogeneous microstructure. For the investigated range of parameters, the composite prepared at 1700 °C for 30 min had the optimum comprehensive mechanical properties with flexural strength of 1121 ± 31 MPa, fracture toughness of 7.9 ± 0.58 MPa·$m^{1/2}$ and hardness of 21.3 ± 0.62 GPa.

(3) The improved flexural strength and fracture toughness of the composite were attributed to the strengthening and toughening effects of Ni and the elongated TiB_2 grains, the intragranular nano-particle structure, and the dislocations and stacking fault. Ni distributed in the interface and triple grain junctions improved the interface bond strength and the relative density of the composite. The *in-situ*-synthesized TiB_2 grains with a diameter of 0.5 – 1.5 μm and an aspect ratio of 3 – 10 improved the flexural strength and fracture toughness of the composite by means of crack deflection, crack bridging, crack branching, grain fracture and grain pullout. The intragranular TiB_2 nanoparticle can not only impede the grain growth of SiC, but also change the fracture mode of the composite. The dislocations and stacking fault can release the stress near the crack tip and enhance the flexural strength. In addition, the clean interface is also conducive to the improved flexural strength of the composite.

Acknowledgements

The work is supported by Jiangsu Key Laboratory of Precision and Micro-Manufacturing Technology (20166398), and Zhejiang Provincial Key Laboratory for Cutting Tools (ZD201603).

References

1 Basu, B., Raju, G.B., Suri, A.K.: Processing and properties of monolithic TiB_2 based materials, *Int. Mater. Rev.*, **51**, 352 – 374, (2006).

2 Yadawa, P.K.: Ultrasonic characterization of ceramic material titanium diboride, *Ceram-Silikaty*, **55**, 127 – 133, (2011).

3 Mukhopadhyay, A., Venkateswaran, T., Basu, B.: Spark plasma sintering may lead to phase instability and inferior mechanical properties: A case study with TiB_2, *Scripta Mater.*, **69**, 159 – 164, (2013).

4 Karthiselva, N.S., Murty, B.S., Bakshi, S.R.: Low temperature synthesis of dense TiB_2 compacts by reaction spark plasma sintering, *Int. J. Refract. Met. Hard Mater.*, **48**, 201 – 210, (2015).

5 Demirskyi, D., Cheng, J., Agrawal, D., Ragulya, A.: Densification and grain growth during microwave sintering of titanium diboride, *Scripta Mater.*, **69**, 610 – 613, (2013).

6 Ferber, M.K., Becher, P.F., Finch, C.B.: Effect of microstructure on the properties of TiB_2 ceramics, *Commun. Am. Ceram. Soc.*, **C**, 2 – 4, (1983).

7 Baca, L., Lences, Z., Jogl, C., Neubauer, E., Vitkovic, M., Merstallinger, A., Sajgalik, P.: Microstructure evolution and tribological properties of TiB_2/Ni-Ta cermets, *J. Eur. Ceram. Soc.*, **32**, 1941 – 1948, (2012).

8 Zhao, G.L., Huang, C.Z., Liu, H.L., Zou, B., Zhu, H.T., Wang, J.: Microstructure and mechanical properties of TiB_2-SiC ceramic composites by reactive hot pressing, *Int. J. Refract. Met. Hard Mater.*, **42**, 36 – 41, (2014).

9 Torizuka, S., Sato, K., Nishio, H., Kishi, T.: Effect of SiC on interfacial reaction and sintering mechanism of TiB_2, *J. Am. Ceram. Soc.*, **78**, 1606 – 1610, (1995).

10 Zhu, D.G., Liu, S.K., Yin, X.D., Yang, L., Xiao, C.C., Zhou, H.M., Zhang, J.Y.: In-situ HIP synthesis of TiB_2/SiC ceramic composites, *J. Mater. Process. Tech.*, **89 – 90**, 457 – 461, (1999).

11 Chen, H.B., Wang, Z., Wu, Z.J.: Investigation and characterization of densification, processing and mechanical properties of TiB_2-SiC ceramics, *Mater. Design*, **64**, 9 – 14, (2014).

12 Zhao, G.L., Huang, C.Z., Liu, H.L., Zou, B., Zhu, H.T., Wang, J.: Microstructure and mechanical properties of hot pressed TiB_2-SiC composite ceramic tool materials at room and elevated temperatures, *Mater. Sci. Eng. A*, **606**, 108 – 116, (2014).

13 Fahrenholtz, W.G.: Reactive processing in ceramic-based systems, *Int. J. Appl. Ceram. Tec.*, **3**, 1 – 12, (2006).

14 Zhang, G.J., Deng, Z.Y., Kondo, N., Yang, J.F., Ohji, T.: Reactive hot pressing of ZrB_2-SiC composites, *J. Am. Ceram. Soc.*, **83**, 2330 – 2332, (2000).

15 Zhang, Z.X., Xu, C.J., Du, X.W., Li, Z.L., Wang, J.L., Xing, W.H., Sheng, Y., Wang, W.M., Fu, Z.Y.: Synthesis mechanism and mechanical properties of TiB_2-SiC composites fabricated with the B_4C-TiC-Si system by reactive hot pressing, *J. Alloys Compd.*, **619**, 26 – 30, (2015).

16 Liu, H.T., Wu, W.W., Zou, J., Ni, D.W., Kan, Y.M., Zhang, G.J.: In situ synthesis of ZrB_2-$MoSi_2$ platelet composites: reac-

tive hot pressing process, microstructure and mechanical properties, *Ceram. Int.*, **38**, 4751 – 4760, (2012).

17 Fahrenholtz, W.G., Loehman, R.E., Ewsuk, K.G.: Reactive hot pressing of alumina-molybdenum disilicide composites, *J. Am. Ceram. Soc.*, **85**, 258 – 260, (2002).

18 Zhao, G.L., Huang, C.Z., Liu, H.L., Zou, B., Zhu, H.T., Wang, J.: A study on in-situ synthesis of TiB_2-SiC ceramic composites by reactive hot pressing, *Ceram. Int.*, **40**, 2305 – 2313, (2014).

19 Fukuhara, M., Fukazawa, K., Fukawa, A.: Physical properties and cutting performance of silicon nitride ceramic, *Wear*, **102**, 195 – 210, (1985).

20 Song, J.P., Huang, C.Z., Zou, B., Liu, H.L., Liu, L., Wang, J.: Effects of sintering additives on microstructure and mechanical properties of TiB_2-WC ceramic-metal composite tool materials, *Int. J. Refract. Met. Hard Mater.*, **30**, 91 – 95, (2012).

21 Evans, A.G.: High toughness ceramics, *Mater. Sci. Eng. A*, **105 – 106**, 65 – 75, (1988).

22 Choi, S.M., Awaji, H.: Nanocomposites-a new material design concept, *Sci. Technol. Adv. Mater.*, **6**, 2 – 10, (2005).